◎ 논 문

DOI: http://dx.doi.org/10.5293/kfma.2012.15.5.060
ISSN (Print): 1226-9883

Study on Surface Vortices in Pump Sump

Ngo Ich Long* · Byeong Rog Shin**† · Deog-Hee Doh***

Key Words : 수중 보텍스 (Submerged vortex), 펌프 흡수정 (Pump sump), 수치해석 (Numerical analysis), 자유 표면 유동 (Free surface Flow), 공기체적 분률 (Air volume fraction), 보텍스 구조 (Vortex structure)

ABSTRACT

One of commonly physical phenomena encountered in pump sump systems in which its significant influence to the hydraulic performance of pump system plays an important role in the field of fluid engineering, is the appearance of free surface and submerged vortices. In this paper, a study of the vortices behavior and their formative mechanism of asymmetry is considered in this paper by using numerical approach. The Reynolds-Averaged Navier-Stokes (RANS) equations and k-omega Shear Stress Transport turbulence model used to describe the properties of turbulent flows, in company with VOF multiphase model, are implemented by Fluent code with multi-block structured grid system. In the numerical simulation, the calculated elevation of air-water interface and vortex core contours are used to classify visually surface vortices as well as submerged vortices. It is shown that the free surface vortex is identified by the concavity of liquid region from the free surface and swirling flow at that own plane. To investigate the distinctive behavior of these vortices corresponding to each given flow rate at the same water level, some numerical testing of them are considered here in such a manner that the flow pattern of surface vortex are obtained similarly to the obtained results from experiment. Furthermore, the influence due to the change of grid refinement and the variation of depth of the concavity are also considered in this paper. From that, these influential factors will be implemented to design a good pump sump with higher performance in the future.

1. Introduction

One of the most important systems in fluid engineering is the pump system with the intake devices designed in accordance with their purpose. In which, the intake devices in sumps play specially an important role to keep stability and uniformity of flow before entering into a pump for improvement of efficiency of pump system. Therefore, the application of intake devices such as a sump type with better models need to be implemented as far as possible. During operating pump system, the unexpected phenomena such as cavitation, head and pressure loss, vibration and noise need to be considered especially in which air-entrained free and submerged vortices appearing in sump pumps will damage seriously to pump system. According to the HI standard of Hydraulic Institute HI [1] or JSME criteria for a pump sump design [2], therefore, these vortices should be prevented as much as possible.

Identifying location, shape, as well as intensity of vortex, is very important in design of pump sump. Therefore to date, studies for the better sump with not only lower cost but higher accuracy has been considered recently by using CFD analysis, one of the effective tools to validate the characteristics of flow around the suction pipes in sump system. An application of a numerical prediction method of a submerged vortex to the flow in pump sumps in order to investigate these vortices was performed by Iwano et al. [3]. In addition, the CFD prediction and model experiment on suction vortices in pump sump was figured out by Okamura et al. [4] by using several CFD commercial codes. Meanwhile S Koshizuka et al. demontrated a feasible method to compute transient fluid flow with free surface [5]. Recently, an experimental and numerical study to investigate detailed behavior of free surface and submerged vortices,

* 창원대학교 대학원 기계공학전공
** 창원대학교 기계공학과, 교신저자
*** 한국해양대학교 기계정보공학부
† 교신저자, E-mail : brshin@changwon.ac.kr

2011 유체기계 연구개발 발표회 발표 논문, 2011년 11월 30일-12월 2일, 경주
유체기계저널:제15권, 제5호, pp. 60~66, 2012(논문접수일자: 2011.10.23, 심사완료일자: 2012.09.08)

minimum water levels incepting the vortices, swirling angle and so on is done by Kang et al. [6].

In this paper, the behavior of free surface and submerged vortices in the model sump system is investigated through some different flow rates at the same either water level or other relative conditions by numerical approach. From that, a process of development of vortex can be confirmed. In this computation, an adaptive mesh in vicinity zone between gas and liquid is used results obtained from the change in flow rate of system and grid refinement are analyzed and discussed in this study.

2. Numerical method

2.1. The testing model

The sump model system was designed according to the recommended layout by HI-9.8 American National Standard for Pump Intake Design as shows in Fig. 1[1]. This model is preceded to divide domain of the entering flow channel into two layers in which water layer and air layer are showed in this figure. Height of water level is equal to 0.3m from the bottom. It is noted that the free surface is assumed as a plat surface at the initial stage (t=0) in this case.

2.2. Numerical methodology

This problem was solved by using the finite volume method of ANSYS FLUENT [7] in which the fundamental equations are the continuity equation and the Reynolds-Averaged Navier-Stokes equations as follows:

$$\frac{\partial \rho}{\partial t}+\frac{\partial}{\partial x_i}(\rho u_i)=0 \quad (1)$$

$$\frac{\partial \rho u_i}{\partial t}+\frac{\partial}{\partial x_j}(\rho u_i u_j)=-\frac{\partial p}{\partial x_i}+\frac{\partial}{\partial x_j}\left[\mu_{eff}\left(\frac{\partial u_i}{\partial x_j}+\frac{\partial u_j}{\partial x_i}\right)\right] \quad (2)$$

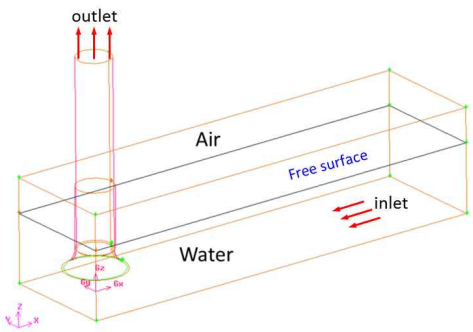

Fig. 1 The geometrical model

Where ρ, u and p and are fluid density, velocity and static pressure, respectively. t is time and μ_{eff} is effective viscosity considered molecular viscosity and turbulent viscosity. A $k-w$ Shear Stress Transport turbulent model [7] and the volume of fluid (VOF) model [8] were used for solving turbulence multiphase flow. Some main features such as computational grid and boundary conditions used in this problem are showed as follows:

2.2.1. Computational grids

In this case, the grid model used for solving discretized equations is generated by Ansys ICEM CFD [9]. Hexahedral mesh is created relatively easy with high quality evaluated by all mesh criteria such as aspect ratio, equiangular skewness or hexahedral quality etc. Furthermore, controlling density of mesh according to required problem, especially at the sensitive region as free surface, is implemented easily through some manipulations with block algorithm. As a result, a multi-block structured grid system with about 870,000 cells of hexahedral mesh was applied as shown in Figs. 2 and 3.

2.2.2. Boundary conditions

The boundary conditions are used in this case by some following main items: The pressure boundary condition is used for inlet of model with pressure distribution conform to the law of hydrostatic; The top surface of air phase are set to pressure boundary condition with given atmospheric pressure; The boundary condition of mass flow rate used for outlet boundary with its respective values, are shown by the Table 1 below; The remaining parts of model are set to no-slip

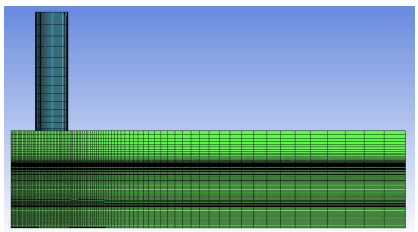

Fig. 2 The grid model in elevation

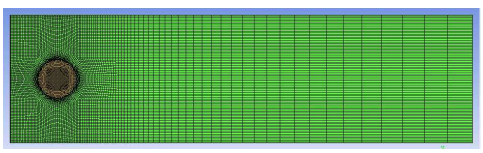

Fig. 3 The grid model in top view

Table 1 The flow rate of outlet boundary

Case	1	2	3	4
Q [m^3/h]	126.9	190.35	219.89	253.8

wall with 60 degree of wall adhesion contact angle recommended from ANSYS FLUENT [7]. In addition, to investigate the influence of grid refinement to the behavior of vortex in pump sump, a fine grid with 4 million elements was experimented.

3. Results and Discussion

The numerical results to investigate the free surface and submerged vortices are shown below by some validating criteria of computer graphics (CG). In which contours of the elevation of air-water interface in Cartesian system and volume fraction describing phase state of fluid are shown through some figures corresponding to each case of volumetric flow rate, as well as of grid refinement. In addition, the statistic results related to the appearance of surface vortex peaks at some computed times will be shown at the end of this section.

3.1. Surface vortices with different flow rate

3.1.1. Case of 126.9 m^3/h volumetric flow rate

In this case, two relatively symmetrical free surface vortices are shown in Figs. 4 and 5 in which the depth of them is about 21mm computed from free surface.

With these two small vortices, the symmetry remains in a long time in this case with 870.000 of mesh. It is conformed that the elevation of the free surface shows a wavy pattern and low water level behind the intake pipe.

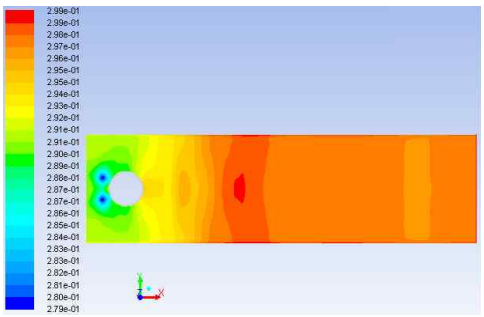

Fig. 4 Elevation of air-water interface at 126.9m^3/h, 10.755s, in top view

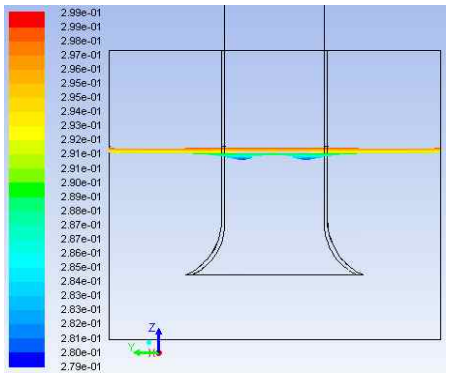

Fig. 5 Elevation of air-water interface at 126.9m^3/h, 10.755s, in front view

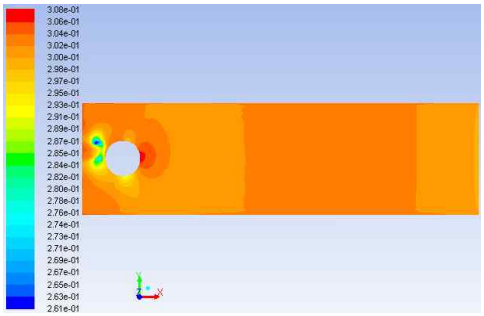

Fig. 6 Elevation of air-water interface at 190.35m^3/h, 19.52s, in top view

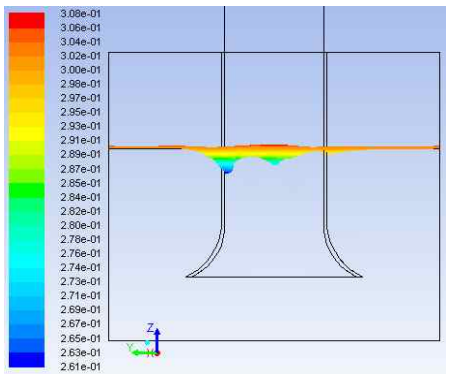

Fig. 7 Elevation of air-water interface at 190.35m^3/h, 19.52s, in front view

3.1.2. Case of 190.35 m^3/h volumetric flow rate

The symmetry of two free surface vortices occurs at the first time (supposed that the impulse process is exceed here). After that, the vortex with greater value in depth (about 39mm) moves gradually to the left side of channel as illustrated clearly in Figs. 6 and 7. It is can be clarified that the asymmetric disturbances generated by a kind of the instability of flow so that the energy of swirl is being transferred

from the asymmetries to the symmetric part through the eddy momentum. it seems that the narrow space behind bell mouth in this case is limited the normal develop of these vortices. And after a stated period of time, the asymmetric disturbances is high enough to move big vortex to a larger space of conners of channel. In addition, the mutual interaction of two vortices also influences to the formation of this asymmetry.

3.1.3. Case of 219.89 m^3/h volumetric flow rate

In this case, when the flow rate is increased continuously, the intensity of swirl flow as well as suction pressure acting on the free surface is increased accordingly. The free surface vortices are therefore formed as shown in Figs. 8 and 9 so that the depth of these surface vortices is greater than previous ones (about 46mm) and their shape of concavity is also similar to tear-drop.

3.1.4. Case of 253.8 m^3/h volumetric flow rate

At this point, the free surface vortices are towards separating easily due to the large flow rate and suction force. That is why many air bubbles fall into water flow and enter into the bell mouth then. This phenomenon can be seen clearly in Figs. 10 and 12 for details. An air bubble is detected inside the intake pipe as shown in Fig. 12. Additionally, to show clearly the air-entrance in sump channel while air bubbles fall into the water flow, air volume fraction is used here with a section plane at vortex center as shown in Fig. 11.

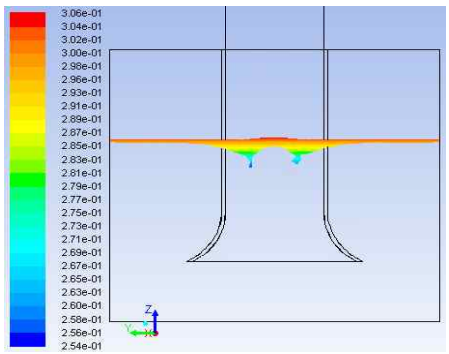

Fig. 8 Elevation of air-water interface at 219.89m^3/h, 8.2s, in front view

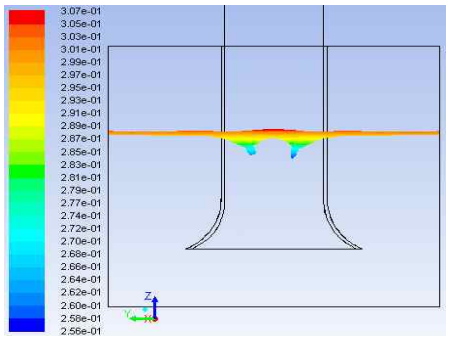

Fig. 9 Elevation of air-water interface at 219.89m^3/h, 9.72s, in front view

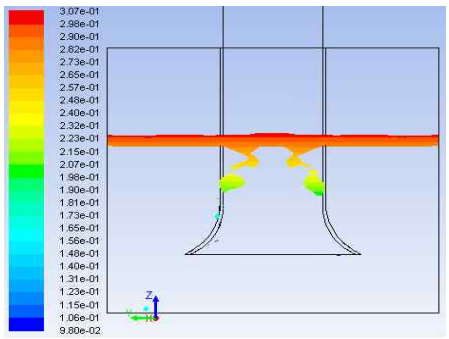

Fig. 10 Elevation of air-water interface at 253.8m^3/h, 8.735s, in front view

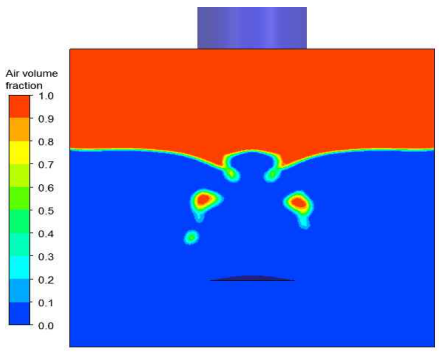

Fig. 11 Contour of air volume fraction at plane-0.12m normal to x direction, 253.8m^3/h, and 8.735s, in front view

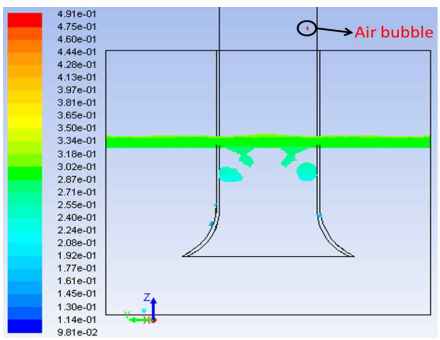

Fig. 12 Elevation of air-water interface at 253.8m^3/h, 8.885s, in front view

3.2. Vortex flow pattern

3.2.1. Grid dependency

Figures 13 and 14 shown time evolution of elevation of air-water interface obtained by using 870.000 grid elements. With time the surface vortex is been developing as seen in Fig. 14. The amplitude of wave of free surface flow is less than 20mm.

In the results with 4 million grid cells, overall it is similar to the previous results in Figs. 13 and 14, however the surface vortex moves asymmetrically at 26.29s as seen in Fig. 16. It implies that the fine mesh can afford to capture small disturbance and the flow instability due to the high resolution. In addition, a number of small air bubble falling into the water flow are more than the of coarse grid with the same boundary conditions.

The influence of grid refinement to shape of concavity of free surface or the depth of that own vortex is seem to be no significance. However either free surface vortex such as its position or the growing number of air bubble falling into the water are somewhat influenced. This is also due to numerical resolution to solve multiphase flow equations including volume fraction equations in general.

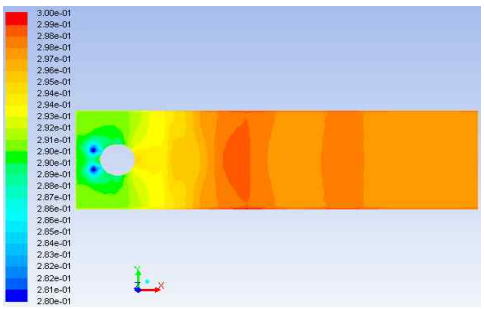

Fig. 13 Elevation of air-water interface at 126.9m³/h, 10.76s, in top view

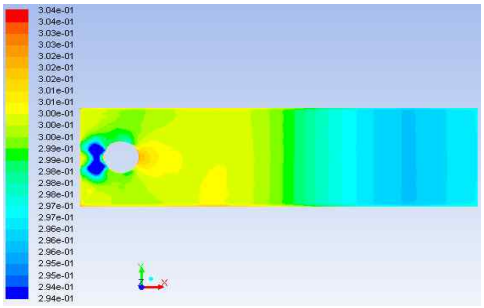

Fig. 14 Elevation of air-water interface at 126.9m³/h, 26.29s, in top view

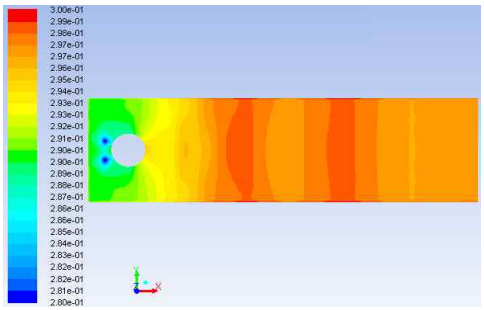

Fig. 15 Elevation of air-water interface at 126.9m³/h, 10.76s, in top view

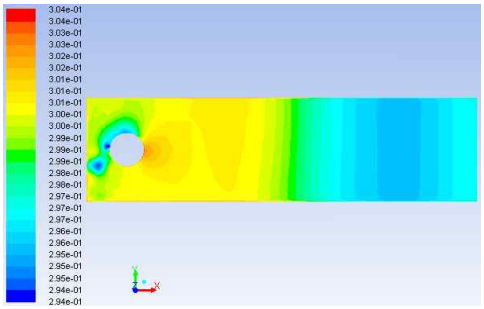

Fig. 16 Elevation of air-water interface at 126.9m³/h, 26.29s, in top view

3.2.2. Surface vortex behavior

Using CG technique is very useful to understand the flow pattern and structures. Figure 17 shows a vortex flow around the intake pipe and bell mouth. Rotating direction and vortex core of free surface and submerged vortices were illustrated in this figure by the voticity vector and equi-surface contours of vortex. These vortices are merged under the bell mouth and discharge through the intake pipe. The free surface flow pattern behind the intake pipe is shown clearly in Fig. 18 by the volume rendering. Especially two free surface vortices with relatively deep concavity and asymmetry between those vortices are illustrated obviously here.

In order to investigate the behavior and development of free surface vortex, the depth of vortex was monitored. Figure 19 shows the depth of free surface vortex with time, by using least-square regression. In which the data of variation of vortex peaks is obtained from computation corresponding to each time step.

Thus, it is clear to show some statements related to the behavior of free surface vortex in terms of depth and flow rate as follows:

-When flow rate is increased gradually from 126.9m³/h to 197.7m³/h, the depth of free surface vortex increases

correspondingly with respect to time between 5s to 50s. The positive slope of fitting line increases and the slope has a maximum value at 190.35m³/h.

−After that, the slope of lines start decreasing gradually until it reaches 219.89 m³/h, the depth of free surface vortex decreases quickly with respect to time due to the break off of the vortex. Simultaneously, the appearance of air bubble falling into the water flow after dropping from free surface vortex also increases. In this situation, the free surface is frequently unstable. This phenomenon is totally similar to that one observed in experimental study about surface vortex in pump sump[6].

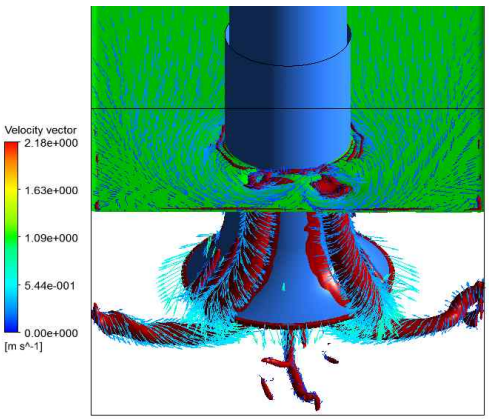

Fig. 17 The free surface and submerged vortices near bell mouth at 126.9m³/h with 4 million cells, in front view

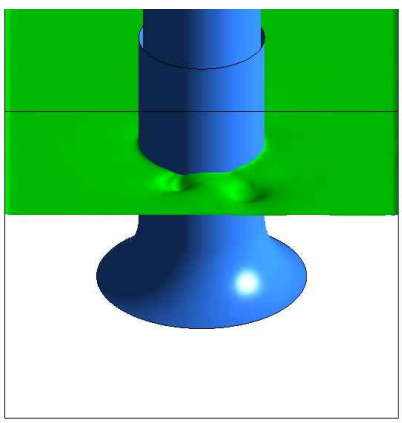

Fig. 18 The flow pattern of free surface at 126.9m³/h with 4 million cells

4. Conclusion

Numerical investigation of behavior of free surface and submerged vortices in pump sump is performed

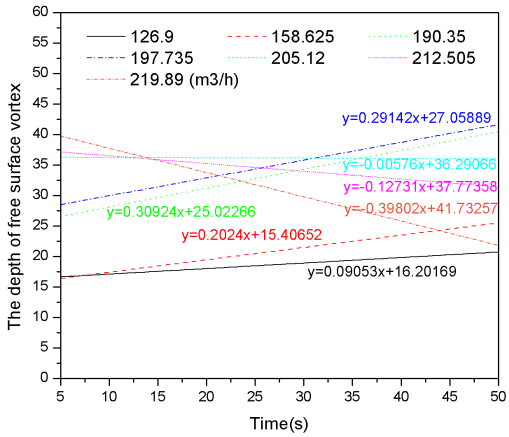

Fig. 19 The variation of free surface vortex

by using RANS equation and k−omega SST turbulent model. A VOF multiphase model included in the Fluent and multi−block structured grid are used. Either type or refinement of adaptive grid and the open channel boundary condition is used to simulate a numerical phenomenon resembling a real test model. In this investigation, a model sump with single flow channel is computed through some different rates at some given water levels. From the results, the unsteady motion of free surface vortices is well simulated similarly to the experimental study. By using the elevation of air−water interface and the measurement of depth of concavity, the behavior of free surface vortices corresponding to each case of given flow rate is well illustrated and clarified. A symmetrical flow pattern at the initial time was changed into an asymmetric one depending on the time so that the free surface vortices move to one arbitrary side of channel due to the flow instability. A relatively common phenomenon in experimental pump sump models in which the very high perturbation of flow caused by air−entrained free and submerged vortices, was also reproduced. When flow rate is increased, the depth of free surface vortex increased with time up to 197.1m³/h, but it decreased gradually from 200m³/h. Through the extraction of the vortex core plane and volume rendering, it was clear the structure of free surface and subsurface vortices. These information of surface vortices will be help to advanced design of pump sump with high performance.

Acknowledgment

This work was supported by the National Research Foundation of Korea (NRF) grant No.2009-0077992, grant No.2009-0083510 funded by the Korean government (MEST) through Multi-phenomena CFD Engineering Research Center and Underwater Vehicle Research Center (UVRC), ADD of Korea.

References

(1) Hydraulic Institute Standard, 1998, American National Standard for Pump Intakes Design, ANSI/HI 9.8.

(2) JSME, 1984, Standard Method for Model Testing the Performance of a Pump Sump, JSME S 004.

(3) Iwano. R., et al., 2002, "Numerical Prediction Method of a Submerged Vortex and Its Application to the Flow in Pump Sump with and without a Baffle Plate," Proc. of 9th Int'l Symposium of Transport Phenomena and Dynamics of Rotating Machinery, pp. 1~6.

(4) Okamura. T., et al., 2007, "CFD Prediction and Model Experiment of Suction Vortices in Pump Sump," Proc. of 9th Asian Int'l Conf. on Fluid Machinery, AICFM9-053.

(5) Koshizuka. S., Tamako. H., and Oka. Y., 1995, A particle method for incompressible viscous flow with fluid fragmentation. Computational Fluid Dynamics, JOURNAL, 4(1): 29-46.

(6) Kang. W. T., et al., 2011, "An investigation of cavitation and suction vortices behavior in pump sump," Proc. of ASME-JSME-KSME Joint Fluid Engineering, AJK2011-33020.

(7) ANSYS group, 2010, FLUENT User's Manual, Version 13.

(8) Hirt. C. W., Nichols, B. D., 1981, "Volume of fluid (VOF) method for the dynamics of free boundaries," Journal of Computational Physics 39 (1): 201-225.

(9) ANSYS group, 2010, ICEM CFD User's Manual, Version 13.